Appendices

Appendix 1: Coordinate systems

Selenographic (SEL) coordinate system

A selenographic coordinate system is a 'simple' coordinate system with a selenocentric origin (centred on the Moon), analogous to the geocentric, geographic coordinate system [Hapgood, 1992]. The *X* axis is the intersection of the zero longitude and the lunar equator, and the *Z* axis is along the rotation axis of the Moon, positive in the direction of angular momentum, with the *Y* axis completing the right-hand set.

The SEL coordinates of *X*, *Y* and *Z* can be related to a spherical coordinate system with co-latitude θ (90°-latitude) and longitude ϕ (in degrees), and radius r (Figure A1.1). The orthogonal vectors $\hat{\mathbf{r}}$, $-\hat{\boldsymbol{\theta}}$ and $-\hat{\boldsymbol{\varphi}}$ point outwards, south and east respectively.

$$X = r\cos\phi\sin\theta$$

$$Y = r\sin\phi\sin\theta$$

$$Z = r\cos\theta$$

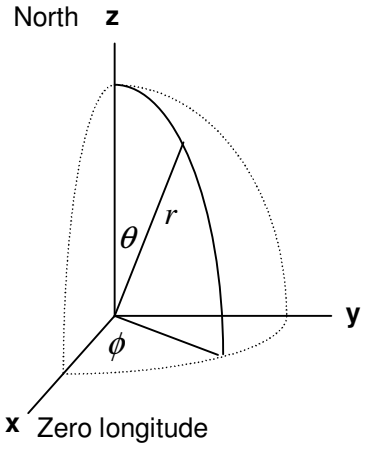

Figure A1.1: Schematic of the SEL and spherical coordinate systems

Magnetic field measurements in SEL coordinates $B_x\ B_y\ B_z$ can easily be converted into local spherical coordinates $B_r\ B_\theta\ B_\phi$ with a simple transformation matrix:

$$\begin{pmatrix} B_r \\ B_\theta \\ B_\varphi \end{pmatrix} = \begin{pmatrix} \sin\theta\cos\phi & \sin\theta\sin\phi & \cos\theta \\ \cos\theta\cos\phi & \cos\theta\sin\phi & -\sin\theta \\ -\sin\phi & \cos\phi & 0 \end{pmatrix} \begin{pmatrix} B_x \\ B_y \\ B_z \end{pmatrix} \qquad \text{(A1.1)}$$

Geocentric Solar Ecliptic (GSE):

This coordinate system is centred on the Earth with the *X* axis the Earth-Sun line, positive towards the Sun, and the *Z* axis directed to the ecliptic north pole (perpendicular to the Sun-Earth plane), and *Y* completes the right-handed set in the ecliptic plane [Hapgood, 1992]. GSE longitude is zero along the Sun line and increases to the east.

Appendix 2: Regional maps of magnetic anomalies

Regional plots of the total magnetic field at A: 30 km altitude from the spherical harmonic model of the lunar crustal magnetic field [Purucker, 2008], and B: at the surface estimated from the ER technique and binned into 1°×1° bins (J.S Halekas, personal communication). Regions are those labelled in figure 2.3. (Plots of the ER data show distortion at higher latitudes.)

Figure overleaf

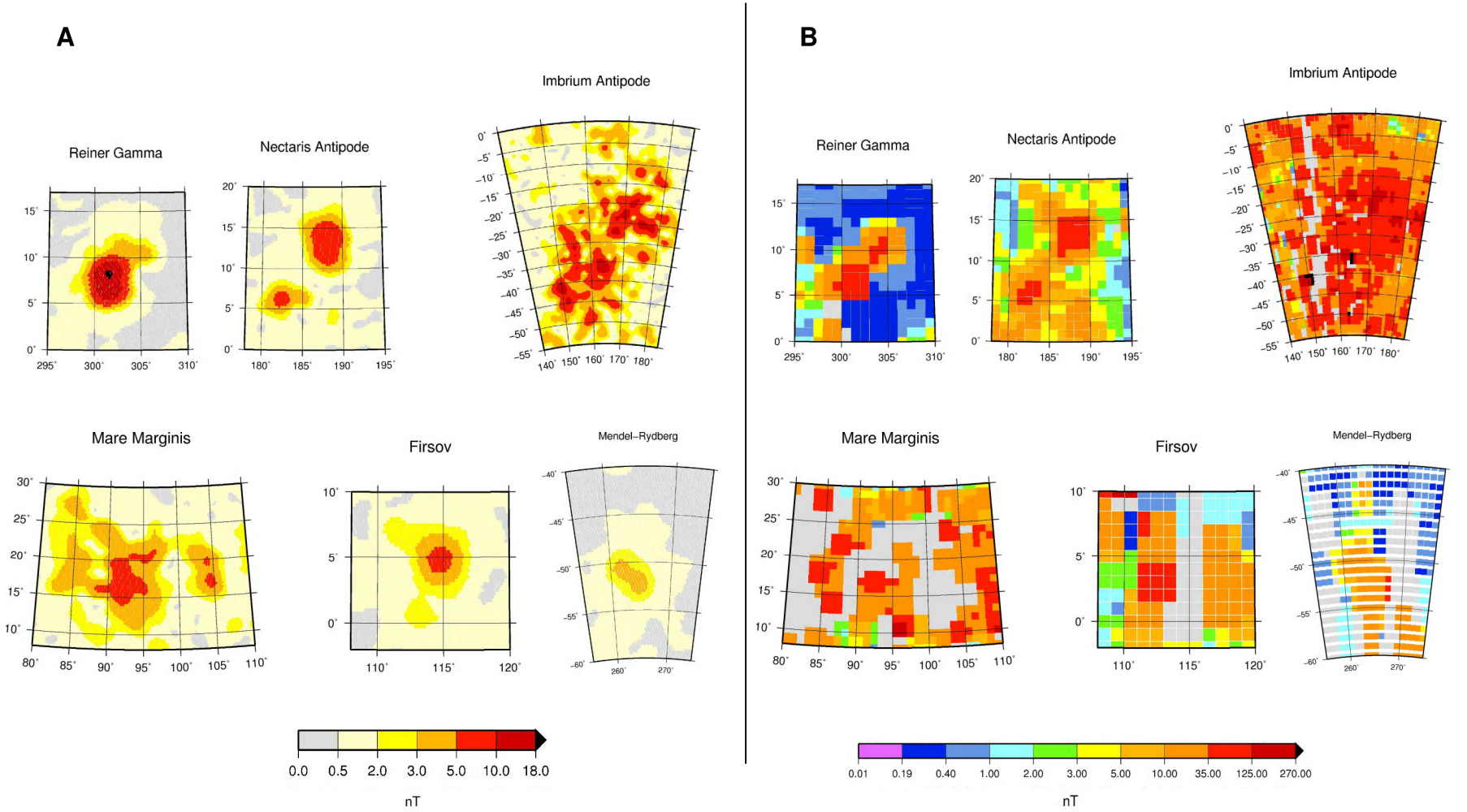
A
Reiner Gamma
Nectaris Antipode
Imbrium Antipode
Mare Marginis
Firsov
Mendel–Rydberg
0.0 0.5 2.0 3.0 5.0 10.0 18.0
nT
B
Reiner Gamma
Nectaris Antipode
Imbrium Antipode
Mare Marginis
Firsov
Mendel–Rydberg
0.01 0.19 0.40 1.00 2.00 3.00 5.00 10.00 35.00 125.00 270.00
nT

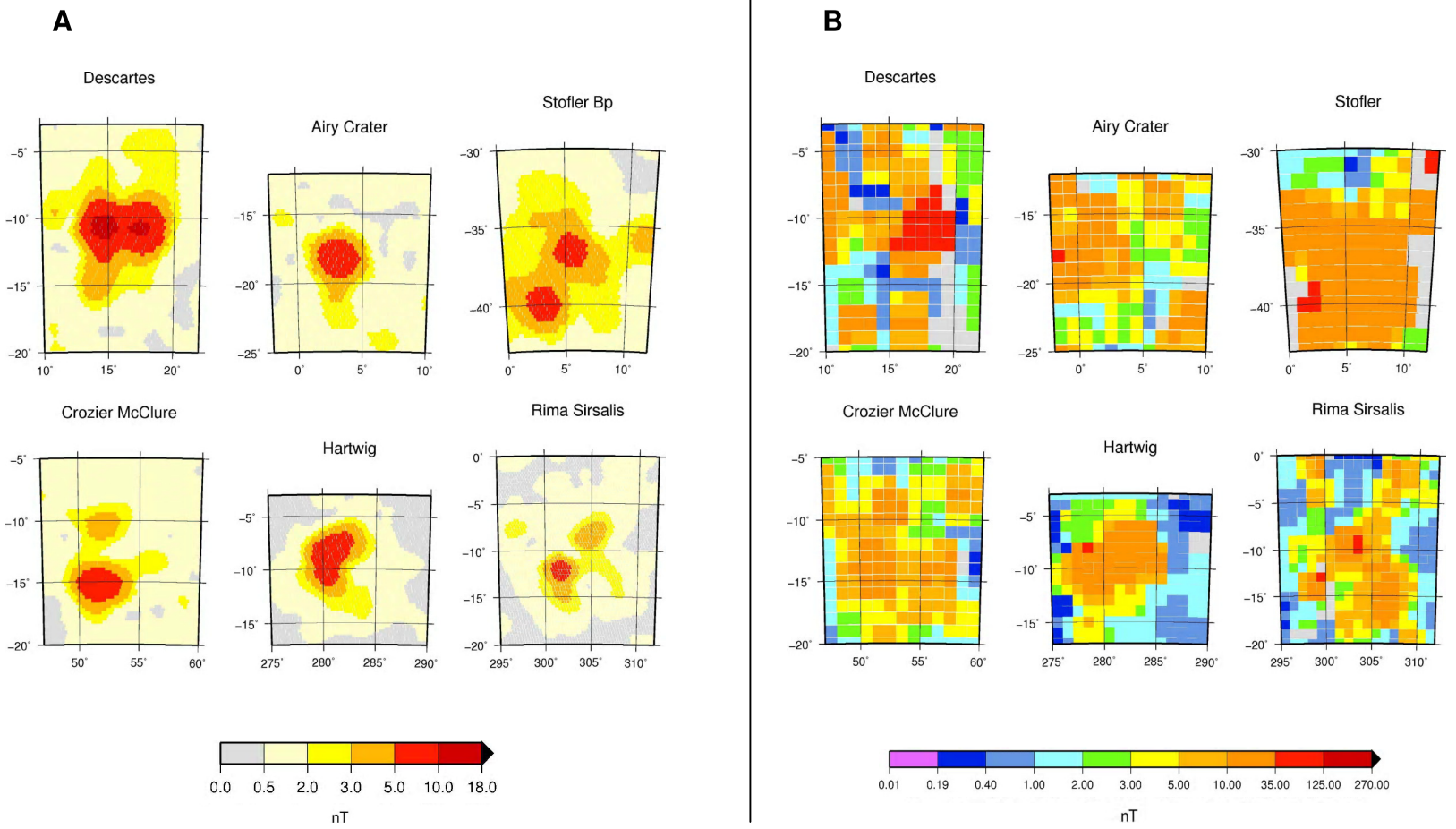
A
Descartes
Airy Crater
Stofler Bp
Crozier McClure
Hartwig
Rima Sirsalis
0.0 0.5 2.0 3.0 5.0 10.0 18.0
nT
B
Descartes
Airy Crater
Stofler
Crozier McClure
Hartwig
Rima Sirsalis
0.01 0.19 0.40 1.00 2.00 3.00 5.00 10.00 35.00 125.00 270.00
nT

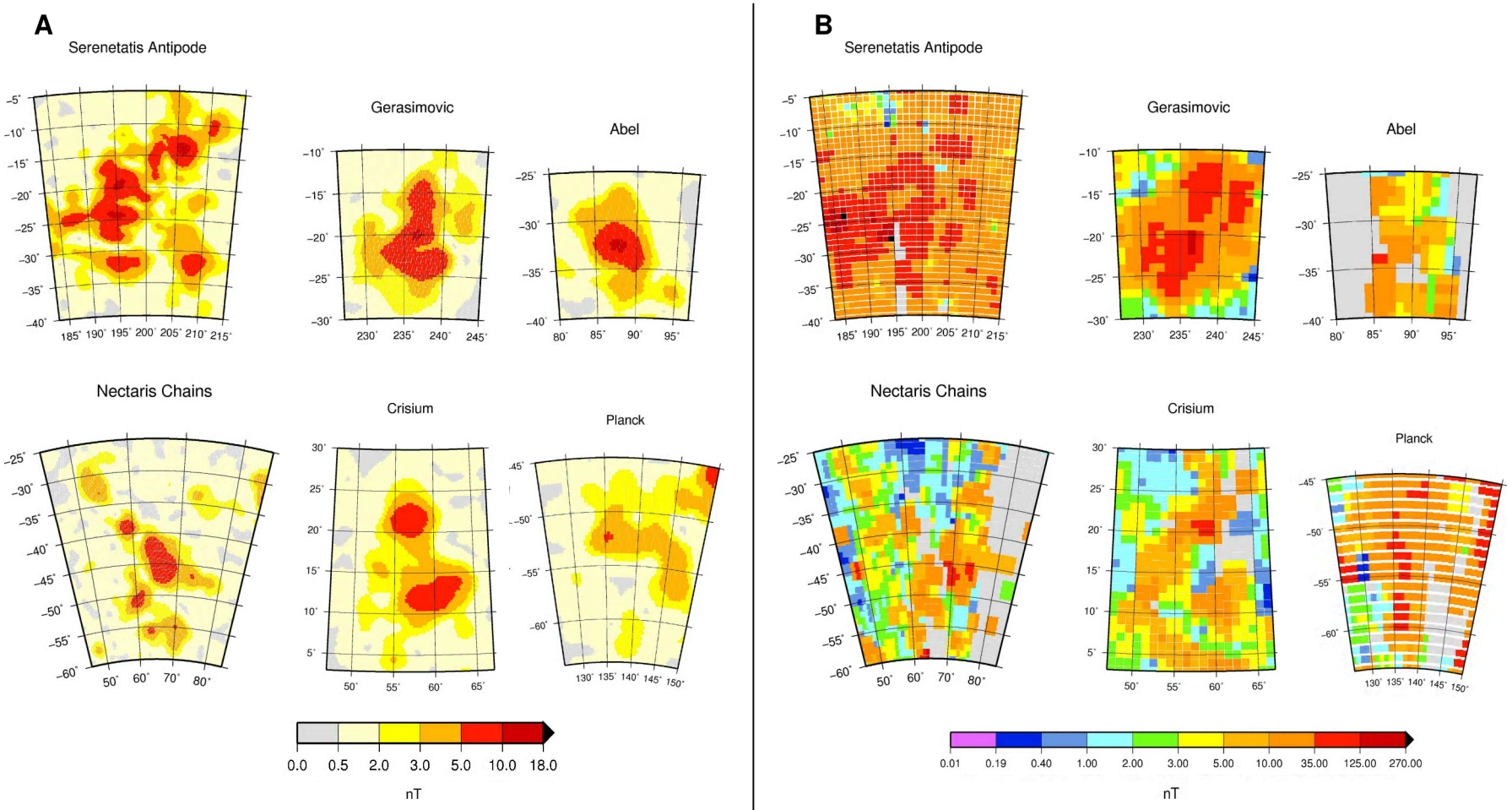
A
Serenetatis Antipode
Gerasimovic
Abel
Nectaris Chains
Crisium
Planck
0.0 0.5 2.0 3.0 5.0 10.0 18.0
nT
B
Serenetatis Antipode
Gerasimovic
Abel
Nectaris Chains
Crisium
Planck
0.01 0.19 0.40 1.00 2.00 3.00 5.00 10.00 35.00 125.00 270.00
nT

Appendix 3: Altitude normalisation

The altitude continuation technique used by Richmond et al. (2005) and Richmond and Hood (2008) applied an inverse power law,

$$B_z = \frac{B_v}{(Z/V)^x} \tag{A3.1}$$

where B_z is the field at constant altitude z, B_v is the field at the spacecraft altitude, and x is a constant which will vary in different regions. The value of x can be determined for a specific region, or as a global average by finding the value for x which successfully continues lower altitude data to higher altitude data. The value of x is between 1 and 3 with a global average of 1.5 [Richmond and Hood, 2008].

Appendix 4: Distribution of points on a sphere

To produce an even distribution (equal area) of points on a spherical surface, a special spherical tessellation is used. Points are located on a sphere using a polar coordinate subdivision [Katanforoush and Shahshahani, 2003] which is superior to icosahedral subdivision, providing a much better distribution of points on a sphere, and is symmetric at the equator (Figure A4.1). Single points are located at the poles, with n_j equally spaced points located on $(n-1)$ equally spaced latitudes, where n_j is given by:

$$n_j = \frac{1}{2} + \sqrt{3}n\cos\phi_j \quad \text{for } \phi_j = \frac{\pi j}{n} - \frac{\pi}{2} \text{ for } j = 1.....(n-1) \qquad \text{(A4.1)}$$

Points on alternate latitudes are shifted by half the spacing of the points on that latitude to make the configuration more symmetric. This distribution has less coverage at the poles and more at the equator but can be rotated to provide more coverage for a region of interest.

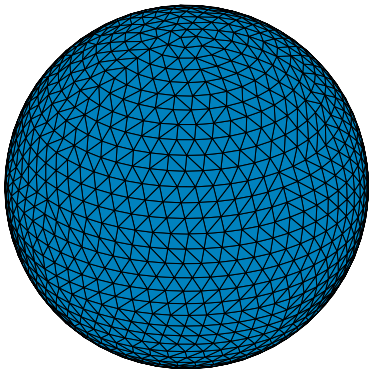

Figure A4.1: A polar coordinate subdivision distribution of points on a sphere.

Appendix 5: Fitting a theoretical power spectrum

Following Voorhies et al. (2002), the fit of a theoretical power spectrum $\{R_n(r)\}$ to the observed power spectrum $R_n(r)$ can be gauged from the sum of squares of residuals s^2 of the log of the powers, and a scatter factor *F*. For degrees from $n_{\min}$ to *N*, fitted with *P* parameters, s^2 for the log of powers, defined by Voorhies et al. (2002) is:

$$s^2 = (N - n_{min} + 1 - P)^{-1} \sum_{n=n_{min}}^{N} [ln(R_n) - ln\{R_n\}]^2 \qquad \text{(A5.1)}$$

The scatter factor *F* (equation A5.2) is the exponential of the RMS residual and is the typical factor by which the theoretical values over or under estimate the observational spectrum for each degree. (*F*=1 would be perfect fit, *F*=2 would be values twice or half the real value).

$$F = e^{\sqrt{s^2 \frac{(N - n_{min} + 1 - P)}{N - n_{min} + 1}}} \qquad \text{(A5.2)}$$

The estimated depth (from r_x), residuals *s*, and scatter factor *F*, for fits to different sections of the spectrum ($n_{\min}$ to $n_{\max}$) are given in table A5.1. For degrees 1-150, the best fitting power spectrum has $A_x = 5.8127 \times 10^{-6}$ and $r_x = 1711.4$ km. The tolerance on this estimation is ~ ± 1 km.

n_{min}	n_{max}	**Depth** (km)	s (nT)	F
1	10	269.547	0.776	2.001
1	20	58.216	0.854	2.248
1	30	28.147	0.722	2.009
1	40	17.186	0.638	1.862
1	50	13.841	0.574	1.755
1	60	14.309	0.527	1.680
1	70	16.801	0.495	1.629
1	80	18.126	0.467	1.586
1	90	19.642	0.446	1.555
1	100	21.512	0.437	1.541
1	110	22.635	0.424	1.522
1	120	23.738	0.415	1.508
1	130	24.562	0.405	1.494
1	140	25.201	0.395	1.481
1	150	25.731	0.387	1.468
140	150	16.958	0.092	1.087
130	150	29.964	0.105	1.105
120	150	29.774	0.095	1.097
110	150	29.511	0.098	1.100
100	150	29.913	0.103	1.106
90	150	29.223	0.102	1.106
80	150	30.362	0.104	1.108
70	150	30.805	0.105	1.110
60	150	30.359	0.109	1.114
50	150	30.469	0.114	1.120
40	150	30.067	0.123	1.130
30	150	29.181	0.145	1.155
20	150	27.707	0.193	1.211
10	150	26.099	0.261	1.296
1	150	25.731	0.387	1.468

Table A5.1: Depth, residuals and scatter factor calculated for theoretical fit to different sections of the observed power spectrum.

Appendix 6: Expression of the magnetic potential

The magnetic potential $\psi_j(\mathbf{r}_i)$, at an observation point $\mathbf{r}_i$ (outside the Moon), arising from a magnetic dipole with magnetic moment $\mathbf{m}_j$ is:

$$\psi_j(\mathbf{r}_i) = \frac{\mu_o}{4\pi}\mathbf{m}_j \cdot \nabla_j \frac{1}{R_{ij}} \tag{A6.1}$$

where ∇_j is the gradient operator (in spherical coordinates) with respect to (r_j, θ_j, ϕ_j). R_{ij} is the distance between the dipole location and the magnetic field observation point which can be defined by the dipole and observation point positions and the angle δ between the two vectors at the centre of the Moon:

$$R_{ij} = \left|\mathbf{r}_i - \mathbf{r}_j\right| = (r_i^2 + r_j^2 - 2r_i r_j \cos\delta)^{1/2} \tag{A6.2}$$

with

$$\cos\delta = \cos\theta_i \cos\theta_j + \sin\theta_i \sin\theta_j \cos(\phi_i - \phi_j) \tag{A6.3}$$

Applying the gradient operator,

$$\begin{aligned}\nabla_j \frac{1}{R_{ij}} = {} & \frac{\partial}{\partial r_j}((r_i^2 + r_j^2 - 2r_i r_j \cos\delta)^{-1/2}) \\ & + \frac{1}{r_j}\frac{\partial}{\partial \theta_j}((r_i^2 + r_j^2 - 2r_i r_j \cos\delta)^{-1/2}) \\ & + \frac{1}{r_j \sin\theta_j}\frac{\partial}{\partial \phi_j}((r_i^2 + r_j^2 - 2r_i r_j \cos\delta)^{-1/2})\end{aligned}$$

$$= \frac{-1}{R_{ij}^3}(r_j - r_i \cos\delta)$$

$$-\frac{1}{R_{ij}^3}(r_i(\cos\theta_i \sin\theta_j - \sin\theta_i \cos\theta_j \cos(\phi_i - \phi_j)))$$

$$+\frac{1}{R_{ij}^3}(r_i \sin\theta_i \sin(\phi_i - \phi_j)) \qquad \text{(A6.4)}$$

Substituting equation A6.4 into equation A6.1 for the potential and using the notation of Dyment and Arkani-Hamed (1998) gives equation 4.4:

$$\psi_j(\mathbf{r}_i) = -\frac{\mu_o}{4\pi}\frac{(m_{j_r}A_1 + m_{j_\theta}B_1 + m_{j_\phi}C_1)}{R_{ij}^3} = -\frac{\mu_o}{4\pi}\frac{m_j(w_r A_1 + w_\theta B_1 + w_\phi C_1)}{R_{ij}^3} \qquad \text{(A6.5)}$$

where

$$A_1 = r_j - r_i \cos\delta$$
$$B_1 = r_i(\cos\theta_i \sin\theta_j - \sin\theta_i \cos\theta_j \cos(\phi_i - \phi_j)) \qquad \text{(A6.6)}$$
$$C_1 = -r_i \sin\theta_i \sin(\phi_i - \phi_j)$$

Appendix 7: Matrix format for equivalent source dipoles

The representation of a set of m observations **B** with n dipoles of magnetisations **m**, through the matrix of linear equations **G**, contains contributions for each dipole and field direction (r, θ, ϕ). The matrix is built up in sections, and the highlighted region shows the contribution of the radial component of the dipoles to the radial component of the field.

$$\mathbf{B} = \mathbf{Gm}$$

$$\begin{pmatrix} B_{r_1} \\ .... \\ B_{r_m} \\ B_{\theta_1} \\ .... \\ B_{\theta_m} \\ B_{\phi_1} \\ .... \\ B_{\phi_m} \end{pmatrix} = \begin{pmatrix} G_{11_{rr}} & ... & G_{1n_{rr}} & G_{11_{r\theta}} & ... & G_{1n_{r\theta}} & G_{11_{r\phi}} & ... & G_{1n_{r\phi}} \\ & \vdots & & & \vdots & & \vdots & & \\ G_{m1_{rr}} & ... & G_{mn_{rr}} & G_{m1_{r\theta}} & ... & G_{mn_{r\theta}} & G_{m1_{r\phi}} & ... & G_{mn_{r\phi}} \\ G_{11_{\theta r}} & ... & G_{1n_{\theta r}} & G_{11_{\theta\theta}} & ... & G_{1n_{\theta\theta}} & G_{11_{\theta\phi}} & ... & G_{1n_{\theta\phi}} \\ & \vdots & & & \vdots & & \vdots & & \\ G_{m1_{\theta r}} & ... & G_{mn_{\theta r}} & G_{m1_{\theta\theta}} & ... & G_{mn_{\theta\theta}} & G_{m1_{\theta\phi}} & ... & G_{mn_{\theta\phi}} \\ G_{11_{\phi r}} & ... & G_{1n_{\phi r}} & G_{11_{\phi\theta}} & ... & G_{1n_{\phi\theta}} & G_{11_{\phi\phi}} & ... & G_{1n_{\phi\phi}} \\ & \vdots & & & \vdots & & \vdots & & \\ G_{m1_{\phi r}} & ... & G_{mn_{\phi r}} & G_{m1_{\phi\theta}} & ... & G_{mn_{\phi\theta}} & G_{m1_{\phi t}} & ... & G_{mn_{\phi\phi}} \end{pmatrix} \begin{pmatrix} m_{r_1} \\ .... \\ m_{r_n} \\ m_{\theta_1} \\ .... \\ m_{\theta_n} \\ m_{\phi_1} \\ .... \\ m_{\phi_n} \end{pmatrix} \quad \text{(A7.1)}$$

Appendix 8: Formation of the normal matrix equations

A solution for $\mathbf{m}$ in $\mathbf{b}+\mathbf{v}=\mathbf{Gm}$ is sought which minimises the sum of squares of the residuals:

$$\begin{aligned}\mathbf{v}^T\mathbf{v} &= \|\mathbf{Gm}-\mathbf{b}\|^2 \\ &= (\mathbf{Gm}-\mathbf{b})^T(\mathbf{Gm}-\mathbf{b}) \\ &= (\mathbf{Gm})^T(\mathbf{Gm})-\mathbf{b}^T(\mathbf{Gm})-(\mathbf{Gm})^T\mathbf{b}+\mathbf{b}^T\mathbf{b} \quad \text{(A8.1)}\end{aligned}$$

where the two middle terms are equal so that,

$$\mathbf{v}^T\mathbf{v} = (\mathbf{Gm})^T(\mathbf{Gm})-2\mathbf{b}^T(\mathbf{Gm})+\mathbf{b}^T\mathbf{b} \quad \text{(A8.2)}$$

Minimising the sum of squares of residuals with respect to the model parameters $\mathbf{m}$,

$$\begin{aligned}&\frac{d}{d\mathbf{m}}((\mathbf{Gm})^T(\mathbf{Gm})-2\mathbf{b}^T(\mathbf{Gm})+\mathbf{b}^T\mathbf{b})=0 \\ &= \mathbf{m}^T\mathbf{G}^T\mathbf{G}+(\mathbf{G}^T\mathbf{Gm})^T-2\mathbf{b}^T\mathbf{G} \quad \text{(A8.3)}\end{aligned}$$

where the first two terms are equal, giving the normal matrix equations as the solution to least squares problem:

$$\begin{aligned}2\mathbf{G}^T\mathbf{Gm}-2\mathbf{G}^T\mathbf{b} &= 0 \\ \mathbf{G}^T\mathbf{Gm} &= \mathbf{G}^T\mathbf{b} \\ \mathbf{m} &= \left[\mathbf{G}^T\mathbf{G}\right]^{-1}\mathbf{G}^T\mathbf{b} \quad \text{(A8.4)}\end{aligned}$$

Appendix 9: The damped least squares solution

Minimisation with respect to the model parameters **m**, of a linear combination of the sum of squares of residuals $\mathbf{v}^T\mathbf{v}$,

$$\mathbf{v}^T\mathbf{v} = (\mathbf{Gm})^T(\mathbf{Gm}) - 2\mathbf{b}^T(\mathbf{Gm}) + \mathbf{b}^T\mathbf{b} \qquad \text{(A9.1)}$$

weighted by a positive Lagrange multiplier $1/\lambda$, and the square of the solution norm, $\mathbf{m}^T\mathbf{m}$, gives:

$$\frac{d}{d\mathbf{m}}\left(\frac{1}{\lambda}\mathbf{v}^T\mathbf{v} + \mathbf{m}^T\mathbf{m}\right) = 0$$

$$\frac{d}{d\mathbf{m}}\left([(\mathbf{Gm})^T(\mathbf{Gm}) - 2\mathbf{b}^T(\mathbf{Gm}) + \mathbf{b}^T\mathbf{b}] + \mathbf{m}^T\mathbf{m}\right) = 0$$

$$\frac{1}{\lambda}(2\mathbf{m}^T\mathbf{G}^T\mathbf{G} - 2\mathbf{b}^T\mathbf{G}) + 2\mathbf{m}^T = 0$$

$$\mathbf{G}^T\mathbf{Gm} + \lambda\mathbf{m} = \mathbf{G}^T\mathbf{b}$$

$$\left[\mathbf{G}^T\mathbf{G} + \lambda\mathbf{I}\right]\mathbf{m} = \mathbf{G}^T\mathbf{b} \qquad \text{(A9.2)}$$

This has the solution:

$$\mathbf{m} = \left[\mathbf{G}^T\mathbf{G} + \lambda\mathbf{I}\right]^{-1}\mathbf{G}^T\mathbf{b} \qquad \text{(A9.3)}$$

The sum of squares of residuals $\mathbf{v}^T\mathbf{v}$, for the damped model solution is given by re-expressing equation A9.1 as

$$\mathbf{v}^T\mathbf{v} = (\mathbf{Gm})^T(\mathbf{Gm}) - \mathbf{b}^T(\mathbf{Gm}) - (\mathbf{Gm})^T\mathbf{b} + \mathbf{b}^T\mathbf{b} \qquad \text{(A9.4)}$$

and substituting for $\mathbf{G}^T\mathbf{b}$ from equation:

$$\mathbf{v}^T\mathbf{v} = (\mathbf{Gm})^T(\mathbf{Gm}) - \mathbf{b}^T(\mathbf{Gm}) - \mathbf{m}^T\left[\mathbf{G}^T\mathbf{G} + \lambda\mathbf{I}\right]\mathbf{m} + \mathbf{b}^T\mathbf{b}$$

$$\mathbf{v}^T\mathbf{v} = (\mathbf{Gm})^T(\mathbf{Gm}) - \mathbf{b}^T(\mathbf{Gm}) - \mathbf{m}^T\mathbf{G}^T\mathbf{Gm} - \lambda\mathbf{m}^T\mathbf{Im} + \mathbf{b}^T\mathbf{b} \qquad \text{(A9.5)}$$

$$\mathbf{v}^T\mathbf{v} = \mathbf{b}^T\mathbf{b} - \mathbf{m}^T\mathbf{G}^T\mathbf{b} - \lambda\mathbf{m}^T\mathbf{m}\,.$$

Appendix 10: Under constrained normal matrix equations

In an under constrained linear inverse problem, the least squares method fails in that there is not a unique solution. An additional constraint of minimum norm combined with the minimum residuals can give a unique solution. Following Menke (1989), a solution $\mathbf{m}$ is found using Lagrange multipliers ($\mathbf{\Lambda}$), which has a minimum norm $\mathbf{m}^T\mathbf{m}$ and also satisfies $\mathbf{v} = \mathbf{b} - \mathbf{G}\mathbf{m} = 0$:

$$\frac{\partial}{\partial \mathbf{m}}(\mathbf{m}^T\mathbf{m} + \mathbf{\Lambda}\mathbf{v}) = 0$$

$$\frac{\partial}{\partial \mathbf{m}}(\mathbf{m}^T\mathbf{m} + \mathbf{\Lambda}(\mathbf{b} - \mathbf{G}\mathbf{m})) = 2\mathbf{m}^T - \mathbf{\Lambda}\mathbf{G} \qquad \text{(A10.1)}$$

$$2\mathbf{m}^T - \mathbf{\Lambda}\mathbf{G} = 0$$

$$2\mathbf{m} = \mathbf{G}^T\mathbf{\Lambda}^T$$

Combining the final result of equation A9.1 with $\mathbf{v} = \mathbf{b} - \mathbf{G}\mathbf{m} = 0$ and solving for $\mathbf{\Lambda}$:

$$\mathbf{b} = \mathbf{G}(\mathbf{G}^T \mathbf{\Lambda}^T/_2)$$

$$\mathbf{\Lambda}^T = 2\left[\mathbf{G}\mathbf{G}^T\right]^{-1}\mathbf{b} \qquad \text{(A10.2)}$$

Substituting $\mathbf{\Lambda}$ into the minimisation $2\mathbf{m} = \mathbf{G}^T\mathbf{\Lambda}^T$ gives:

$$2\mathbf{m} = 2\mathbf{G}^T\left[\mathbf{G}\mathbf{G}^T\right]^{-1}\mathbf{b}$$

$$\mathbf{m} = \mathbf{G}^T\left[\mathbf{G}\mathbf{G}^T\right]^{-1}\mathbf{b} \qquad \text{(A10.3)}$$

Appendix 11: Formulations for the continuous magnetisation model

Following the notation in Appendix B of Jackson (1990), equation 5.7 can be expressed as:

$$\Gamma_{ik}^{(gp)} = \left(\frac{\mu_o}{4\pi}\right)^2 (\hat{\mathbf{I}}_i^{(p)} \cdot \nabla_i)(\hat{\mathbf{I}}_k^{(g)} \cdot \nabla_k) \int_V \nabla_i F_i \cdot \nabla_k F_k \, dV \qquad \text{(A11.1)}$$

where $F_i = \frac{1}{|\mathbf{r}_i - \mathbf{s}|}$ and we have utilised $\nabla_s \frac{1}{|\mathbf{r}_i - \mathbf{s}|} = -\nabla_i \frac{1}{|\mathbf{r}_i - \mathbf{s}|}$.

The volume integral of equation A11.1 can be re-expressed as:

$$\nabla_i F_i \cdot \nabla_k F_k = \nabla_i \cdot (F_i \nabla_k F_k) - F_i \nabla_k \nabla_i F_k \qquad \text{(A11.2)}$$

where the last term is equal to zero since the observation locations r_k are outside of the magnetised volume. Applying Gauss's theorem, the volume integral can be expressed as a surface integral,

$$\int_V \nabla_i \cdot (F_i \nabla_k F_k) dV = \int_s F_i \nabla_k F_k \cdot \hat{\mathbf{n}}(\mathbf{s}) dS = \int_s \frac{1}{|\mathbf{r}_i - \mathbf{s}|} \frac{\partial}{\partial r} \left(\frac{1}{|\mathbf{r}_k - \mathbf{s}|} \right) dS \qquad \text{(A11.3)}$$

where $\hat{\mathbf{n}}$ is the normal to the surface at *s*. This integral has to be performed over both the inner and outer spheres of the crustal layer, at radii *a* and *a-t*.

The integrals are carried out using the Legendre polynomials $P_n(\mu_k)$, where μ_k is the cosine of the angle between r_k and *s* and

$$\frac{1}{|\mathbf{r}_k - \mathbf{s}|} = \frac{1}{s}\sum_{n=0}^{\infty}\left(\frac{s}{r_k}\right)^{n+1} P_n(\mu_k) \tag{A11.4}$$

Using the addition theorem for complex fully normalised spherical harmonics,

$$P_l(\mu_k) = \frac{4\pi}{2l+1}\sum_{m=-l}^{l} Y_l^m(\theta,\phi) Y_l^{m*}(\theta_k,\phi_k) \tag{A11.5}$$

equation A11.3 can be written quite simply as

$$\int_V \nabla_i F_i \cdot \nabla_k F_k \, dV = \frac{4\pi}{s} Q(\mu_{ik}, \rho) \tag{A11.6}$$

where

$$Q(\mu,\rho) = \sum_{l=0}^{\infty} \frac{l}{2l+1} \rho^{l+1} P_l(\mu) \tag{A11.7}$$

and μ_{ik} is the cosine of the angle between the vectors r_i and r_k , and $\rho = \frac{s^2}{r_i r_k}$ with s being the radius of the sphere of integration (the inner and outer spheres of the crustal layer).

Inputting equation A11.6 into equation A11.1, the elements of the Gram matrix are:

$$\Gamma_{ik}^{(gp)} = \left(\frac{\mu_o}{4\pi}\right)^2 (\hat{\mathbf{I}}_i^{(p)} \cdot \nabla_i)(\hat{\mathbf{I}}_k^{(g)} \cdot \nabla_k)\left[\frac{4\pi}{s} Q\right] \tag{A11.8}$$

which requires derivatives of Q with respect to the component directions of the magnetic field data. A complicated version of the chain rule allows the derivatives of Q with respect to ρ and μ to be calculated.

To carry out these derivatives, the infinite sum in Q needs to be put in closed form. Jackson (1990) used elliptical integrals to express the elements of $\mathbf{\Gamma}$ in closed form resulting in exact, yet complicated functions (Appendix B, Jackson 1990).

These can be approximated when the magnetised layer of thickness *t* is thin (the ratio $\varepsilon = t/a$ is small) so that equation A11.7 becomes

$$Q(\mu,\rho) = \sum_{l=0}^{\infty} \frac{l}{2l+1} \rho^{l+1} \left[1 - (1-\varepsilon)^{2l+1} \right] P_l(\mu) \qquad \text{(A11.9)}$$

and equation A11.8 becomes

$$\Gamma_{ik}^{(gp)} = \left(\frac{\mu_o}{4\pi} \right)^2 (\hat{\mathbf{I}}_i^{(p)} \cdot \nabla_i)(\hat{\mathbf{I}}_k^{(g)} \cdot \nabla_k) \left[\frac{4\pi}{a} Q \right] \qquad \text{(A11.10)}$$

where now $\rho = \dfrac{a^2}{r_i r_k}$ [Whaler and Langel, 1996]. Keeping the first three terms of the expansion $(1-\varepsilon)^{2l+1}$, and using the approximation that $1 - l\varepsilon \approx e^{-l\varepsilon}$, equation A11.9 becomes

$$\sum_{l=0}^{\infty} \frac{\varepsilon}{\gamma} l (\gamma\rho)^{l+1} P_l(\mu) \qquad \text{(A11.11)}$$

Where $\gamma = e^{-\varepsilon}$. This can be more easily put in closed form using the generating function for spherical harmonics. The required derivatives of *Q*, and hence the Gram matrix elements, can be expressed straightforwardly in terms of elementary functions of ρ and μ using the value γ (In Appendix B, Whaler and Langel, 1996). Approximations of the matrix elements agree well with the exact calculated values but can be replaced by the exact values when $\mu = \pm 1$ (concentric and antipodal points) for improved accuracy.

Appendix 12: Damped least squares solution for the continuous magnetisation model

Similarly to appendix 9, minimisation with respect to the model solution $\boldsymbol{\alpha}$, of a linear combination of the sum of squares of residuals S^2,

$$S^2 = (\mathbf{B} - \boldsymbol{\Gamma}\boldsymbol{\alpha})^T (\mathbf{B} - \boldsymbol{\Gamma}\boldsymbol{\alpha}) \tag{A12.1}$$
$$S^2 = (\boldsymbol{\Gamma}\boldsymbol{\alpha})^T (\boldsymbol{\Gamma}\boldsymbol{\alpha}) - 2\mathbf{B}^T (\boldsymbol{\Gamma}\boldsymbol{\alpha}) + \mathbf{B}^T\mathbf{B}$$

weighted by a positive Lagrange multiplier $1/\lambda$, and the square of the solution norm $\boldsymbol{\alpha}^T\boldsymbol{\Gamma}\boldsymbol{\alpha}$, gives:

$$\frac{\partial}{\partial \boldsymbol{\alpha}}(\boldsymbol{\alpha}^T\boldsymbol{\Gamma}\boldsymbol{\alpha} + 1/\lambda[(\mathbf{B} - \boldsymbol{\Gamma}\boldsymbol{\alpha})^T (\mathbf{B} - \boldsymbol{\Gamma}\boldsymbol{\alpha}) - S^2]) = 0$$
$$= 2\boldsymbol{\Gamma}^T\boldsymbol{\alpha} + 1/\lambda[2\boldsymbol{\Gamma}^T\boldsymbol{\Gamma}\boldsymbol{\alpha} - 2\boldsymbol{\Gamma}^T\mathbf{B}] \tag{A12.2}$$
$$2\boldsymbol{\Gamma}^T(\boldsymbol{\alpha} + 1/\lambda\,\boldsymbol{\Gamma}\boldsymbol{\alpha}) = 2/\lambda\,\boldsymbol{\Gamma}^T\mathbf{B}$$
$$\boldsymbol{\Gamma}^T(\lambda\mathbf{I} + \boldsymbol{\Gamma})\boldsymbol{\alpha} = \boldsymbol{\Gamma}^T\mathbf{B}$$

As the Green's functions are linearly independent, the Gram matrix is non-singular and so there exists an inverse, giving:

$$\mathbf{B} = (\boldsymbol{\Gamma} + \lambda\mathbf{I})\boldsymbol{\alpha} \tag{A12.3}$$

Appendix 13: Magnetisation solutions for selected regions

The three component magnetisation solutions for the regions labelled in figure 2.3, from the spatially continuous magnetisation model with layer thickness of 30 km and damping parameter 20,000.

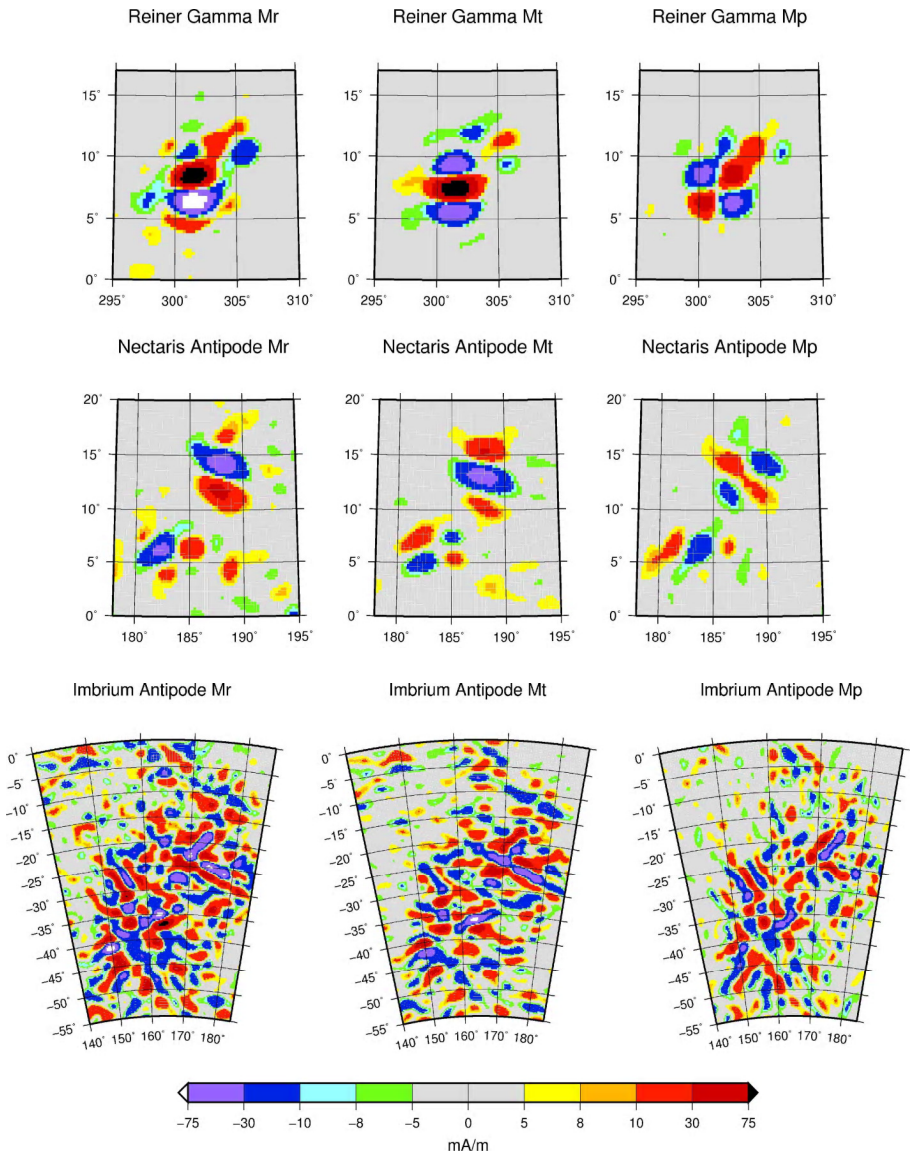

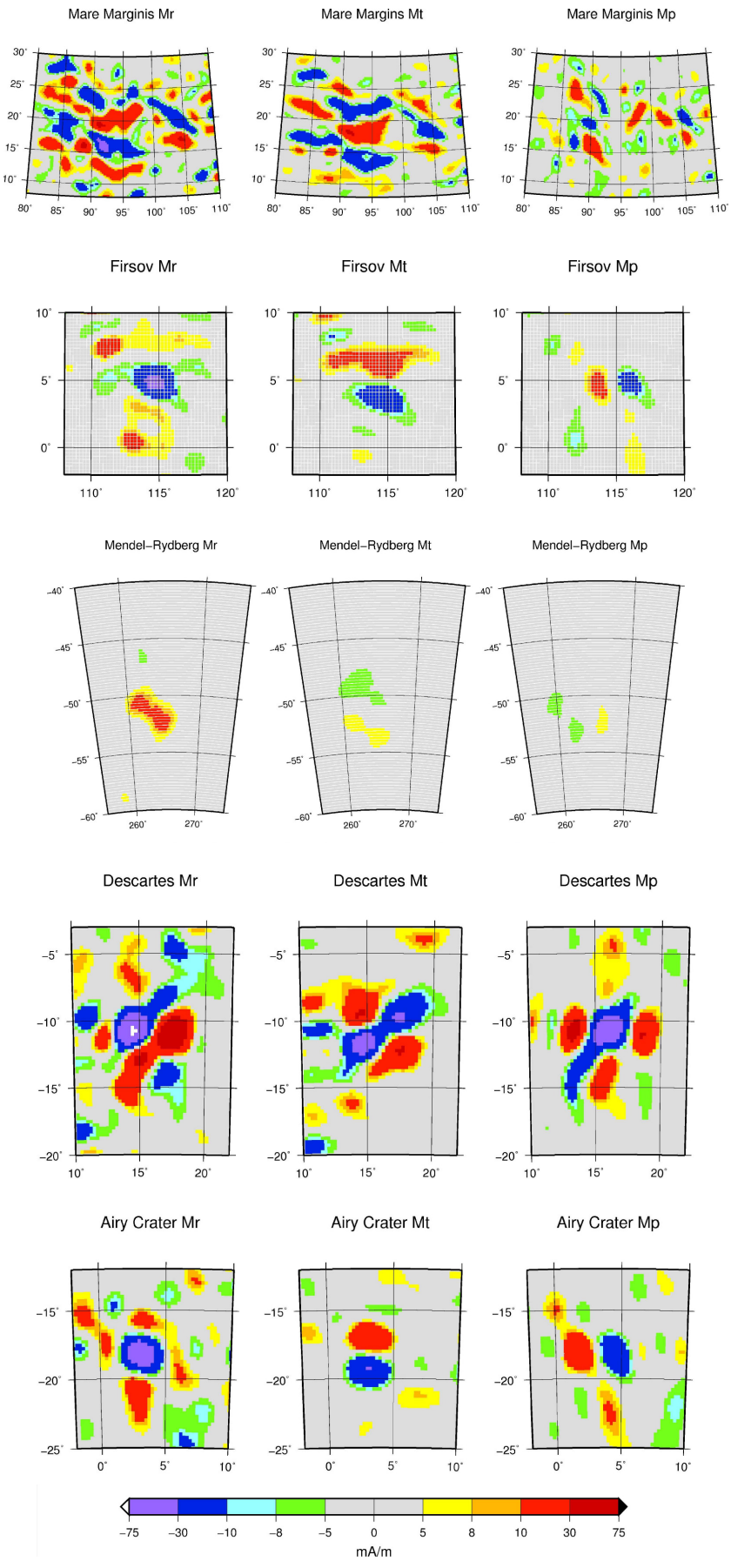
Mare Marginis Mr
Mare Margins Mt
Mare Marginis Mp
Firsov Mr
Firsov Mt
Firsov Mp
Mendel–Rydberg Mr
Mendel–Rydberg Mt
Mendel–Rydberg Mp
Descartes Mr
Descartes Mt
Descartes Mp
Airy Crater Mr
Airy Crater Mt
Airy Crater Mp
−75 −30 −10 −8 −5 0 5 8 10 30 75
mA/m

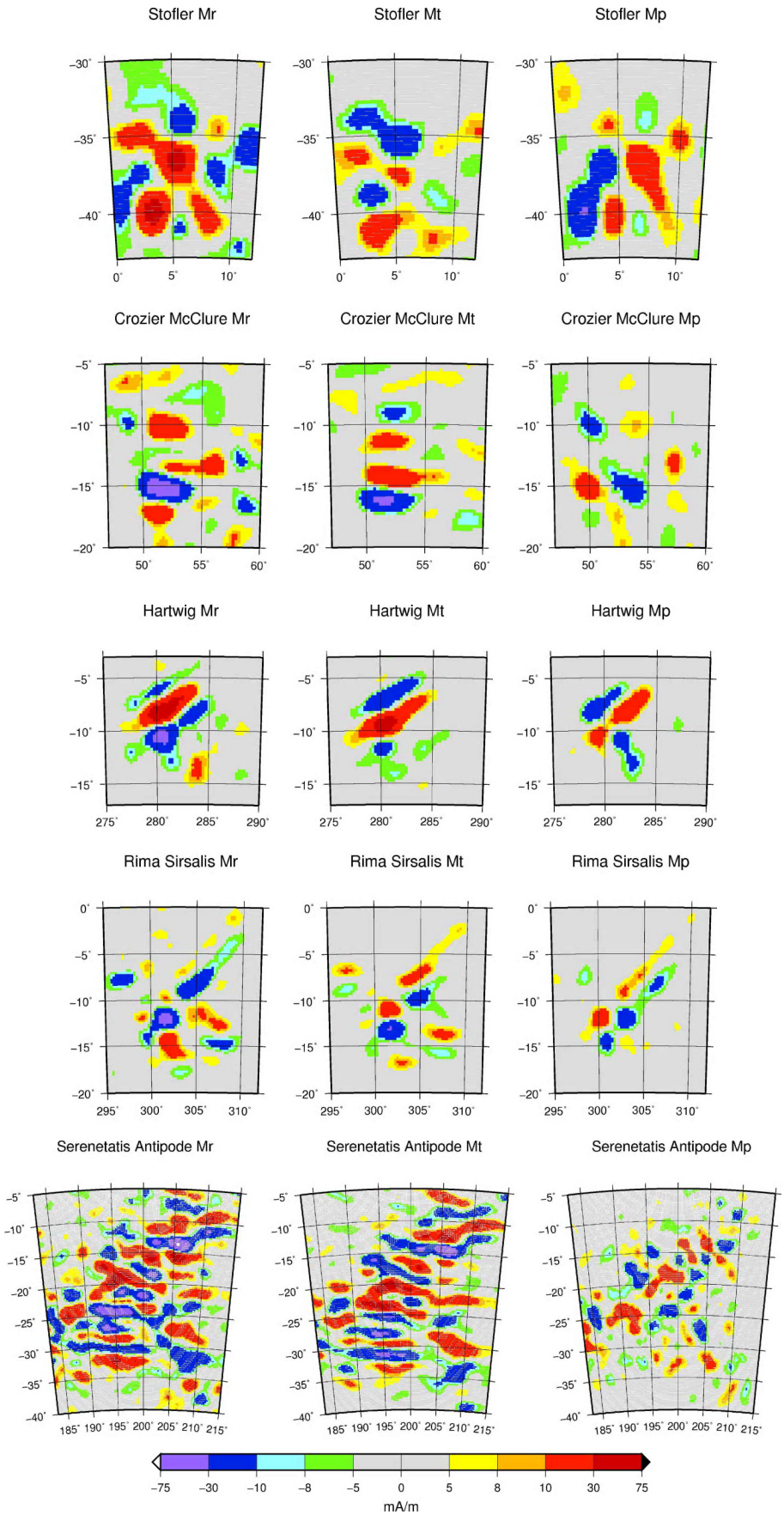
Stofler Mr
Stofler Mt
Stofler Mp
Crozier McClure Mr
Crozier McClure Mt
Crozier McClure Mp
Hartwig Mr
Hartwig Mt
Hartwig Mp
Rima Sirsalis Mr
Rima Sirsalis Mt
Rima Sirsalis Mp
Serenetatis Antipode Mr
Serenetatis Antipode Mt
Serenetatis Antipode Mp
−75 −30 −10 −8 −5 0 5 8 10 30 75
mA/m

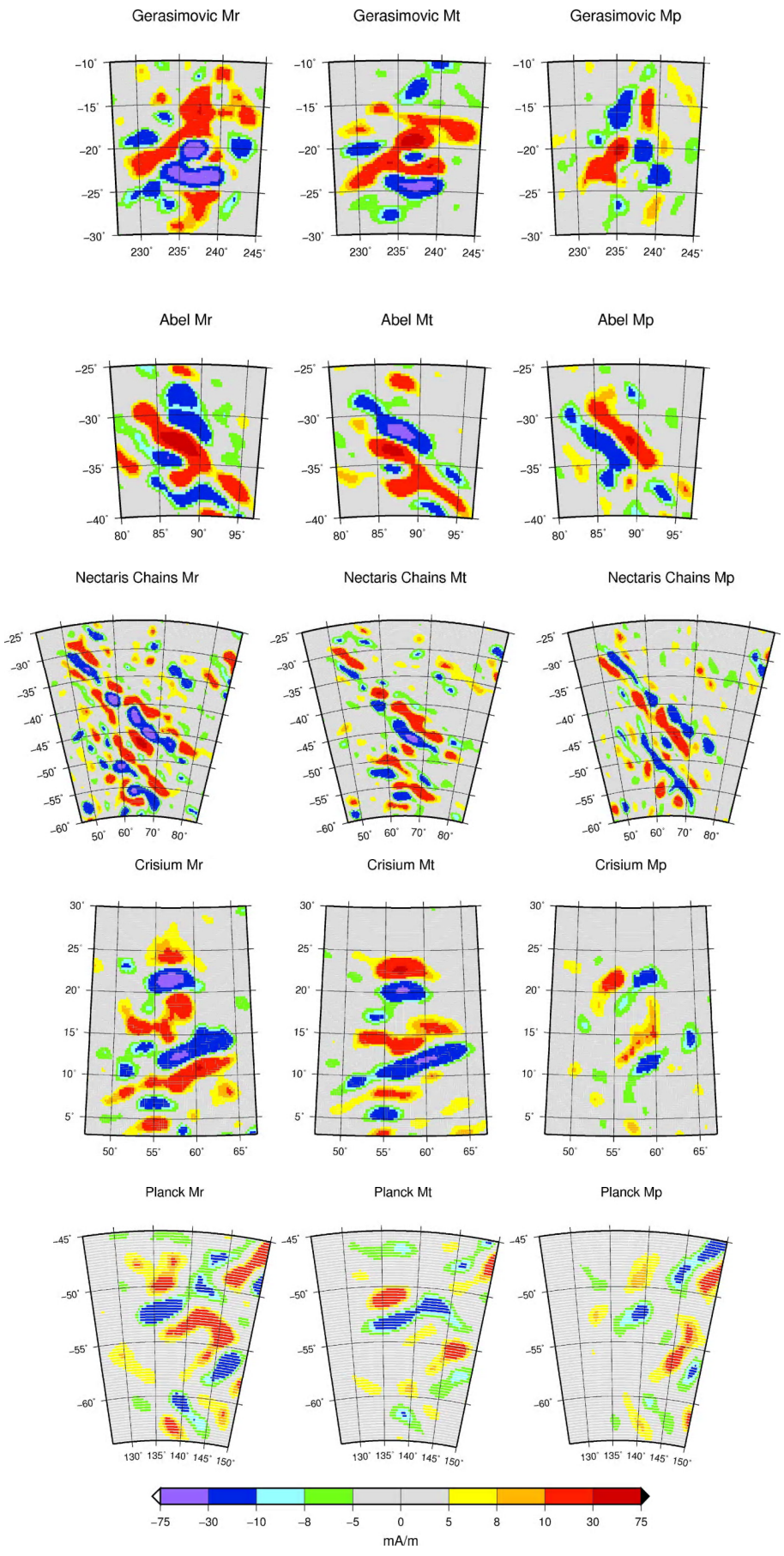
Gerasimovic Mr
Gerasimovic Mt
Gerasimovic Mp
Abel Mr
Abel Mt
Abel Mp
Nectaris Chains Mr
Nectaris Chains Mt
Nectaris Chains Mp
Crisium Mr
Crisium Mt
Crisium Mp
Planck Mr
Planck Mt
Planck Mp
−75 −30 −10 −8 −5 0 5 8 10 30 75
mA/m

Appendix 14: Regional surface predictions from a spatially continuous model

The predicted surface fields at the 1°×1° binned ER locations for the regions labelled in figure 2.3, from the spatially continuous global magnetisation model with layer thickness of 10 km and damping parameter 15,000.

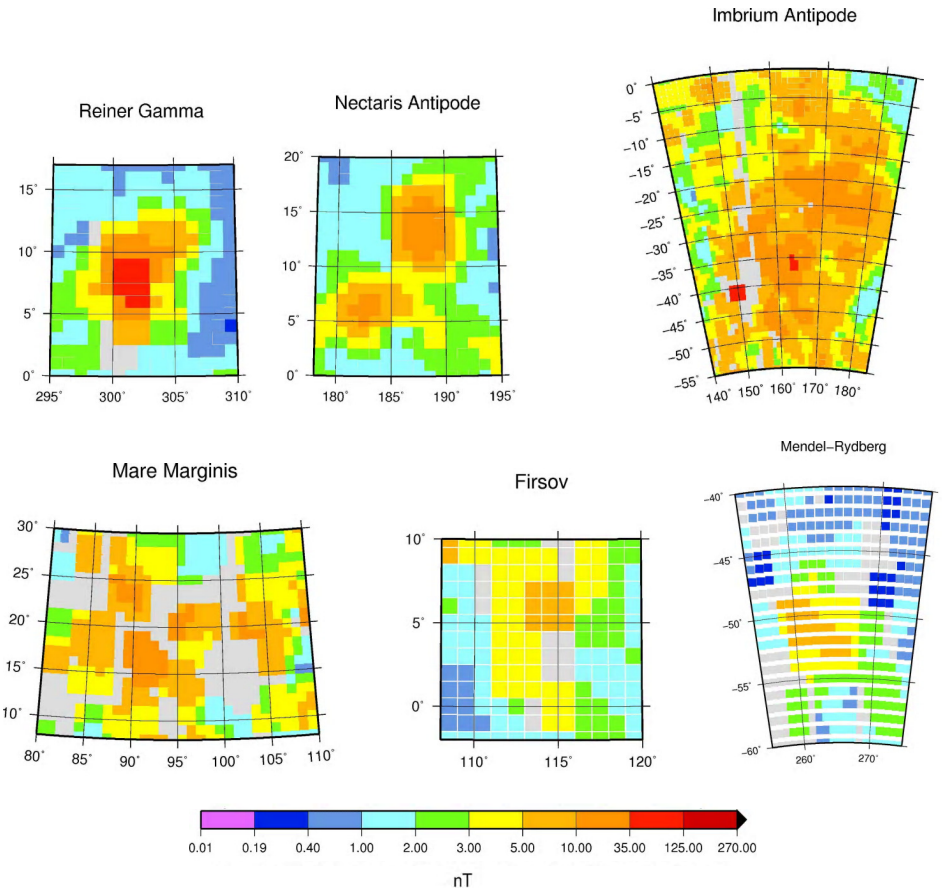

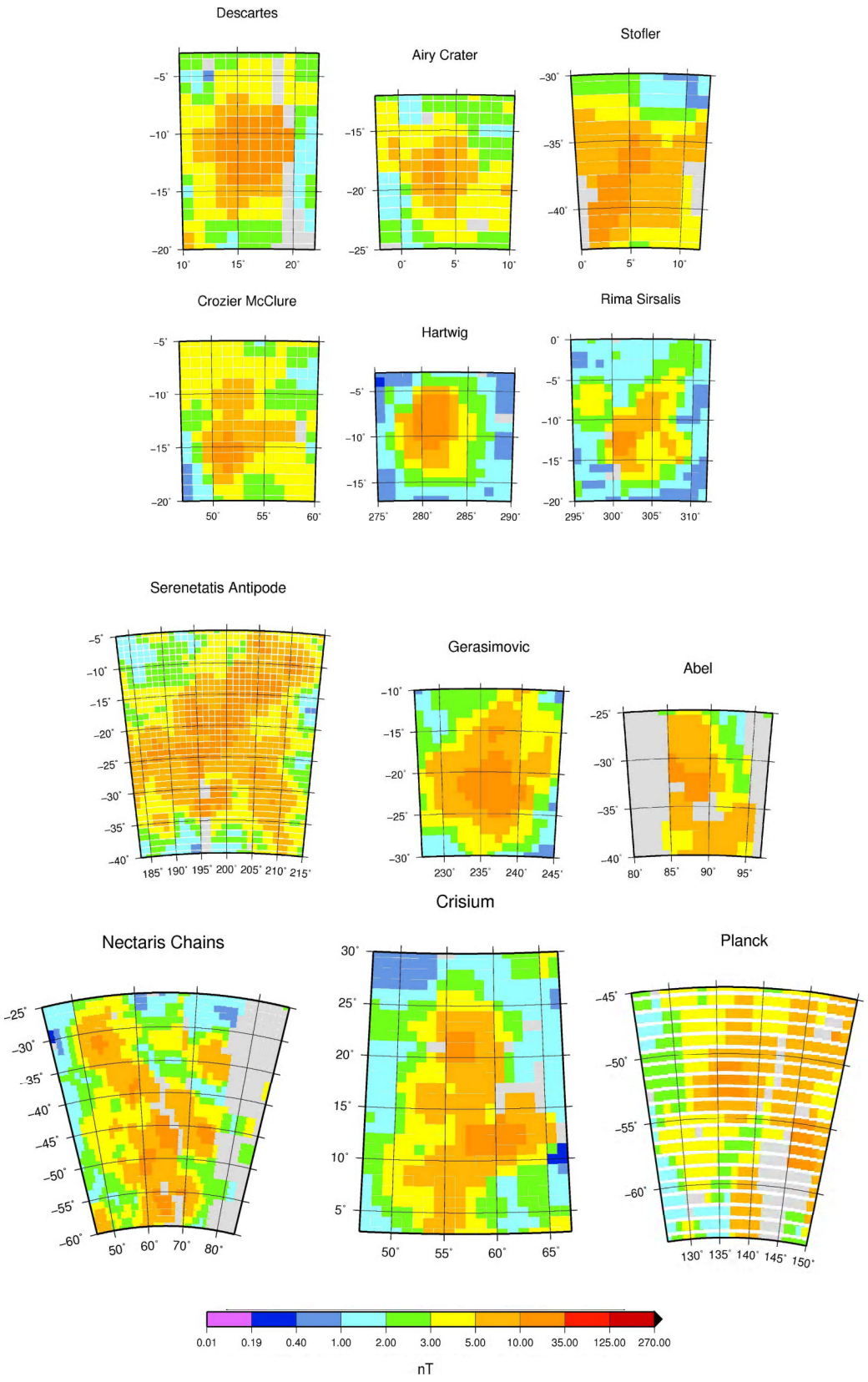
Descartes
Airy Crater
Stofler
Crozier McClure
Hartwig
Rima Sirsalis
Serenetatis Antipode
Gerasimovic
Abel
Crisium
Nectaris Chains
Planck
0.01 0.19 0.40 1.00 2.00 3.00 5.00 10.00 35.00 125.00 270.00
nT

Appendix 15: Simplification of joint matrix multiplication

For a matrix **J**, of size (M×N), with $M = mx + my$, the product $\mathbf{J}^T\mathbf{J}$ expressed as:

$$\left[\mathbf{J}^T\mathbf{J}\right]_{ij} = J_{i,1}^T J_{1,j} + J_{i,2}^T J_{2,j} + ...J_{i,M}^T J_{M,j} = \sum_{k=1}^{M} J_{ki} J_{kj} \tag{A15.1}$$

can be split into parts:

$$\left[\mathbf{J}^T\mathbf{J}\right]_{ij} = \sum_{k=1}^{mx} J_{ki} J_{kj} + \sum_{l=mx+1}^{my} J_{li} J_{lj} \tag{A15.2}$$

so that

$$\mathbf{J}(z) = \begin{pmatrix} \mathbf{G} \\ -- \\ \mathbf{P}\big|_{\mathbf{m}(z)} \end{pmatrix} \tag{A15.3}$$

can be simplified into:

$$\mathbf{J}^T(z)\mathbf{J}(z) = \mathbf{G}^T\mathbf{G} + \mathbf{P}\big|_{\mathbf{m}(z)}^T \mathbf{P}\big|_{\mathbf{m}(z)} \tag{A15.4}$$